IMPLEMENTING MULTI-SCALE AGRICULTURAL INDICATORS EXPLOITING SENTINELS

VEGETATION FIELD DATA AND PRODUCTION OF GROUND-BASED MAPS:

"CAPITANATA SITE, ITALY" 18TH MARCH AND 13TH MAY, 2014

ISSUE I1.00

EC Proposal Reference N° FP7-311766

Actual submission date : May 2016

Start date of project: 01.11.2012   Duration : 40 months

Name of lead partner for this deliverable: EOLAB

Book Captain: Consuelo Latorre (EOLAB)

Contributing Authors: F. Camacho (EOLAB)

A. Castrignanò, D. De Benedetto, A.M. Stellacci, D. Ventrella, P. Campi (CRA-SCA)
M. Rinaldi, C. Maddaluno, M. Mucci(CRA-CER)
A. Matese, P. Toscano (CNR-IBIMET)

Project co-funded by the European Commission within the Seventh Framework Program (2007-2013)		
Dissemination Level		
PU	Public	**X**
PP	Restricted to other programme participants (including the Commission Services)	
RE	Restricted to a group specified by the consortium (including the Commission Services)	
CO	Confidential, only for members of the consortium (including the Commission Services)	

DOCUMENT RELEASE SHEET

Book Captain:	C. Latorre	Date: 31.05.2016	Sign.
Approval:	R. Lacaze	Date: 17.06.2016	Sign.
Endorsement:	M. Koleva	Date:	Sign.
Distribution:	Public		

CHANGE RECORD

Issue/Revision	Date	Page(s)	Description of Change	Release
	31.05.2016	All	First Issue	I1.00

TABLE OF CONTENTS

LIST OF FIGURES

LIST OF TABLES

LIST OF ACRONYMS

CEOS	Committee on Earth Observation Satellite
CEOS LPV	Land Product Validation Subgroup
CER	Cereal Research Centre (Italy)
CNR	*Consiglio Nazionale delle Ricerche* - National Research Council (Italy)
CRA	Council for Agricultural Research and Agricultural Economy Analysis (Italy)
DG AGRI	Directorate General for Agriculture and Rural Development
DG RELEX	Directorate General for External Relations (European Commission)
ECV	Essential Climate Variables
EUROSTATS	Directorate General of the European Commission
ESU	Elementary Sampling Unit
FAPAR	Fraction of Absorbed Photo-synthetically Active Radiation
FAO	Food and Agriculture Organization
GCOS	Global Climate Observing System
GEO-GLAM	Global Agricultural Geo- Monitoring Initiative
GIO-GL	GMES Initial Operations - Global Land (GMES)
GCOS	Global Climate Observing System
GMES	Global Monitoring for Environment and Security
GPS	Global Positioning System
IBIMET	Institute of Biometeorology
IMAGINES	Implementing Multi-scale Agricultural Indicators Exploiting Sentinels
ISAFOM	Istituto per i sistemi Agricoli e Forestali del Mediterraneo
JECAM	Joint Experiment for Crop Assessment and Monitoring
LAI	Leaf Area Index
LDAS	Land Data Assimilation System
LUT	Look-up-table techniques
PROBA-V	Project for On-Board Autonomy satellite, the V standing for vegetation.
RMSE	Root Mean Square Error
SPOT /VGT	Satellite Pour l'Observation de la Terre / VEGETATION
SCA	Unità di Ricerca per I Sistemi Colturali degli Ambienti caldo-aridi**SCI** GMES Services Coordinated Interface
SLT	Solar Local Time
TOA	Top of Atmosphere Reflectance
USGS	U.S. Geological Survey Science organization.
UTM	Universal Transverse Mercator coordinates system
VALERI	Validation of Land European Remote sensing Instruments
WGCV	Working Group on Calibration and Validation (CEOS)

1. BACKGROUND OF THE DOCUMENT

1.1. EXECUTIVE SUMMARY

The Copernicus Land Service has been built in the framework of the FP7 geoland2 project, which has set up pre-operational infrastructures. ImagineS intends to ensure the continuity of the innovation and development activities of geoland2 to support the operations of the global land component of the GMES Initial Operation (GIO) phase. In particular, the use of the future Sentinel data in an operational context will be prepared. Moreover, IMAGINES will favor the emergence of new downstream activities dedicated to the monitoring of crop and fodder production.

The main objectives of ImagineS are to (i) improve the retrieval of basic biophysical variables, mainly LAI, FAPAR and the surface albedo, identified as Terrestrial Essential Climate Variables, by merging the information coming from different sensors (PROBA-V and Landsat) in view to prepare the use of Sentinel missions data; (ii) develop qualified software able to process multi-sensor data at the global scale on a fully automatic basis; (iii) complement and contribute to the existing or future agricultural services by providing new data streams relying upon an original method to assess the above-ground biomass, based on the assimilation of satellite products in a Land Data Assimilation System (LDAS) in order to monitor the crop/fodder biomass production together with the carbon and water fluxes;(iv) demonstrate the added value of this contribution for a community of users acting at global, European, national, and regional scales.

Further, ImagineS serves the growing needs of international (e.g. FAO and NGOs), European (e.g. DG AGRI, EUROSTATS, DG RELEX), and national users (e.g. national services in agro-meteorology, ministries, group of producers, traders) on accurate and reliable information for the implementation of the EU Common Agricultural Policy, of the food security policy, for early warning systems, and trading issues. ImagineS will also contribute to the Global Agricultural Geo-Monitoring Initiative (GEO-GLAM) by its original agriculture service which can monitor crop and fodder production together with the carbon and water fluxes and can provide drought indicators, and through links with JECAM (Joint Experiment for Crop Assessment and Monitoring).

1.2. PORTFOLIO

The ImagineS portfolio contains global and regional biophysical variables derived from multi-sensor satellite data, at different spatial resolutions, together with agricultural indicators, including the above-ground biomass, the carbon and water fluxes, and drought indices resulting from the assimilation of the biophysical variables in the Land Data Assimilation System (LDAS).

The production in Near Real Time of the 333m resolution products, at a frequency of 10 days, using PROBA-V data is carried out in the Copernicus Global Land Service. (http://land.copernicus.eu/global/).

The demonstration of high resolution (30m) products derived from Landsat-8 was done over demonstration sites of cropland and grassland in contrasting climatic and environmental conditions. Demonstration products are available on the ImagineS website (http://www.fp7-imagines.eu/pages/services-and-products/landsat-8-biophysical-products.php).

1.3. SCOPE AND OBJECTIVES

The main objective of this document is to describe the field campaign and ground data collected at Capitanata, in Italy, and the up-scaling of the ground data to produce ground-based high resolution maps of the following biophysical variables:

- Leaf Area Index (LAI), defined as half of the total developed area of leaves per unit ground surface area (m^2/m^2). We focused on two different LAI quantities (for green elements):
  - ➢ The effective LAI (LAIeff) derived from the description of the gap fraction as a function of the view zenith angle.
  - ➢ The actual LAI (LAI) estimate corrected from the clumping index.
- Fraction of Absorbed Photosynthetically Active Radiation (FAPAR), which is the fraction of the photosynthetically active radiation (PAR) absorbed by a vegetation canopy. We are also focused on green elements. PAR is the solar radiation reaching the canopy in the 0.4–0.7 µm wavelength region. FAPAR was estimated from LAI measurements using the Beer's law, and empirical coefficients.

1.4. CONTENT OF THE DOCUMENT

This document is structured as follows:

- Chapter 2 provides an introduction to the field experiment.
- Chapter 3 provides the location and description of the site.
- Chapter 4 describes the ground measurements, including material and methods, sampling and data processing.
- Chapter 5 provides an evaluation of the sampling.
- Chapter 6 describes the production of high resolution ground-based maps, and the selected "mean" values for validation.

2. INTRODUCTION

Validation of remote sensing products is mandatory to guaranty that the satellite products meets the user's requirements. Protocols for validation of global LAIeff products are already developed in the context of Land Product Validation (LPV) group of the Committee on Earth Observation Satellite (CEOS) for the validation of satellite-derived land products (Fernandes et al., 2014), and recently applied to Copernicus global land products based on SPOT/VGT observations (Camacho et al., 2013). This generic approach is made of 2 major components:

- The indirect validation: including inter-comparison between products as well as evaluation of their temporal and spatial consistency
- The direct validation: comparing satellite products to ground measurements of the corresponding biophysical variables. In the case of low and medium resolution sensors, the main difficulty relies on scaling local ground measurements to the extent corresponding to pixels size. However, the direct validation is limited by the small number of sites, for that reason a main objective of ImagineS is the collection of ground truth data in demonstration sites.

The content of this document is compliant with existing validation guidelines (for direct validation) as proposed by the CEOS LPV group (Morisette et al., 2006); the VALERI project (http://w3.avignon.inra.fr/valeri/) and ESA campaigns (Baret and Fernandes, 2012). It therefore follows the general strategy based on a bottom up approach: it starts from the scale of the individual measurements that are aggregated over an elementary sampling unit (ESU) corresponding to a support area consistent with that of the high resolution imagery used for the up-scaling of ground data. Several ESUs are sampled over the site. Radiometric values over a decametric image are also extracted over the ESUs. This will be later used to develop empirical transfer functions for up-scaling the ESU ground measurements (e.g. Martínez et al., 2009). Finally, the high resolution ground based map will be compared with the medium resolution satellite product at the spatial support of the product.

One of the JECAM sites, "Italy Apulian Tavoliere" is located in Capitanata area, Italy. The experimental farm is managed by CNR-SCA (*Consiglio Nazionale delle Ricerche - Unità di Ricerca per I Sistemi Colturali degli Ambienti caldo-aridi*).

During 2014, two field campaigns were carried out in March and May. A set of ground-truth LAI measurements, soil and crop type data were collected in order to: 1) calibrate a simulation model of crop growth and production and 2) implement a data fusion method aimed at integration of remote sensing data with ground-based measurements (JECAM, 2014).

This report describes the ground dataset and the up-scaling processing performed by EOLAB over the ground dataset provided by CRA-SCA corresponding to the following campaigns:

Field Campaigns:

- **First campaign:** 18th to 20th of March, 2014
- **Second campaign:** 9th to 13th of May, 2014

Contact:

- CRA – SCA Bari: Annamaria Castrignanò, Daniela De Benedetto, Domenico Ventrella, Anna Maria Stellacci and Pasquale Campi.

- CRA-CER Foggia: Michele Rinaldi, Carmen Maddaluno and Massimo Mucci.

- CNR-IBIMET Florence: Alessandro Matese and Piero Toscano.

3. STUDY AREA

3.1. LOCATION

The field campaign was located on the "Capitanata area", a plain of about 4000 km^2 located in the northern part of Apulia Region (south-eastern Italy), province of Foggia (Figure 1). Capitanata plain is delimited by the Apennines Chain west and by Gargano Promontory east and is mostly constituted by continental and fluvial sediments and some terraced marine deposits of the Pliocene and Pleistocene ages.
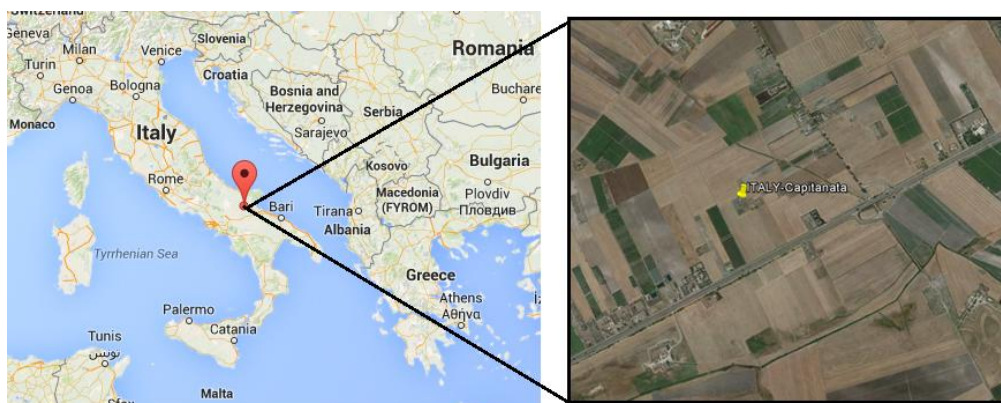
Figure 1: Location of Capitanata site in Italy.

Table 1: Coordinates and altitude of the test site (centre).

CAMPAIGN	Altitude	Latitud	Longitude
Capitanata	90m	41.4637º N	+15.4867º E

Figure 2 shows the false color composition (RGB – SWIR-NIR-RED) over a Top Of Atmosphere (TOA) Reflectance Landsat-7 images used for up-scaling the ground dataset. Few clouds are observed in the acquisition of March.
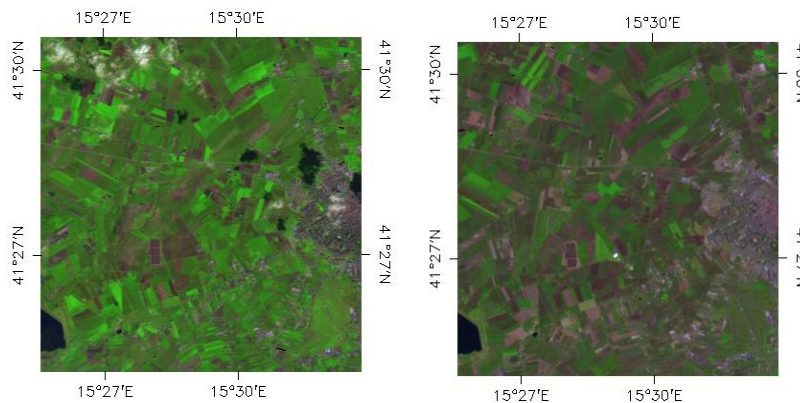
Figure 2: False color composition (SWIR-NIR-RED) of TOA Reflectance Landsat-7 images over the study area 10 km^2. (Capitanata, 18th March and 13th May, 2014).

3.2. DESCRIPTION OF THE TEST SITE

This area is characterized by farms with average size up to 20 ha, highly productive soils cultivated under intensive and irrigated regime. Winter durum wheat (Triticum durum L.) represents the main cereal crop often grown in rotations with irrigated horticultural species . Among these, processing tomato crop (Lycopersicon aesculentum Mill.) is well represented. In particular, two-year rotation (tomato-wheat) and three – year rotation (tomato-wheat-wheat) are the typical rotations of this important productive area (JECAM, 2014). Figure 3 shows a picture of Capitanata landscape.

The climate of this zone is classified as "Accentuated Thermo- Mediterranean" (UNESCO-FAO), with winter seasons characterized by temperatures that sometimes descend below 0°C and hot summers with temperature that may exceed 40°C. Annual precipitation ranges between 400 and 800 mm, mostly concentrated in winter months. The rainiest months are October and November, while the dry period is from May to September. In general, the soils are deep and clay with vertical behaviour, characterized by large and deep cracks in summer season under rain fed conditions. A wide part of the area is served by an irrigation consortium that fulfils the water requirements of crops with spring-summer cycle (e.g. tomato). In other parts, the irrigation for spring crops is carried out by utilizing private wells. The water table is very deep (200-300 m) (JECAM, 2014).

**Figure 3: Landscape picture of Capitanata site (Italy). (*Picture courtesy of JECAM)*

Figure 4 shows a trial area and a landscape of Capitanata where the Meteorological Station is located on the Farm.

Figure 4: Pictures taken during the field campaigns (March, 2014) in Capitanata site (Italy). Left: Trial area. Right: Meteorological Station. (JECAM report 2014).

4. GROUND MEASUREMENTS

The ground measurement database reported here was acquired by several groups from Italy: CNR-SCA, CRA-CER and CNR-IBIMET.

4.1. MATERIAL AND METHODS

Effective LAI (LAIeff): Effective Leaf area index (LAIeff) is defined as the total one-sided leaf area per unit ground surface area (m^2 m^{-2}). LAIeff was measured with LAI-2000 Plant Canopy Analyzer (LI-COR Inc., 2013) (See 4.1.1) which uses a fish-eye lens with a hemispheric field of view (± 45°). The detector is composed of five concentric rings (sensitive to radiation in the 320-490 nm range). Each ring responds over a different range of zenith angles and radiation is thus azimuthally integrated. The measurements were collected in one sensor mode using a 45° view cap, in clear sky condition, to avoid interferences from users' shadow.

This equipment measures the LAIeff by means of gap fraction, using above and below canopy light measurements.

LAI: The actual LAI that can be measured only with a planimeter with however possible allometric relationships to reduce the sampling, is related to the effective leaf area index through:

$$LAI_{eff} = C_f \cdot LAI \qquad \text{Eq. (1)}$$

where C_f is the clumping index (Lang, 1986 and 1987), (Nilson, 1971).

The LAIeff was used to derive the clumpling factor (C_f) using an empirical relationship for the study area based on the modified Beer's law (Rinaldi and Garofalo, 2011). In order to apply the Eq.2, a light extinction coefficient (k) defined as the slope of regression between the natural logarithm of diffuse non-intercepted sky radiation and LAI was calculated, both measured with a LI-COR LAI 2000 (*k* value resulted = 0.75).

$$Cf = k + (0.25) * \left(1 - e^{(-0.35*LAI_{eff})}\right) \qquad \text{Eq. (2)}$$

Intercepted PAR: The photosynthetic active radiation (PAR) intercepted by the canopy was estimated using the following equation:

$$iPAR = PAR \cdot IE \qquad \text{Eq. (3)}$$

Global solar radiation (Rg 300-2500 nm) was derived from a pyranometer located in the local climatic station using the value recorded at the same time when the LAI was measured. PAR is equal to 0.48xRg

FAPAR: As there is little scattering by leaves in that particular spectral domain due to the strong absorbing features of the photosynthetic pigments, FAPAR is often assumed to be equal to FIPAR (Fraction of Intercepted Photosynthetically Active Radiation), and therefore directly related to the gap fraction. The FIPAR was estimated according to Rinaldi and Garofalo, (2011), where IE is the interception efficiency of the canopy, calculated with Beer's law, as:

$$IE = FIPAR = 1 - e^{(k*LAI_{eff}*Cf)}$$ Eq. (4)

The coefficient of extinction (k) and the clumping (Cf) were derived as described above.

*The following data is provided in the associated file: Effective LAI, LAI, Cf (clumping factor), FAPAR, Solar Global Radiation (Rg), PAR, among other information related to the stage and description of the ESUs. The uncertainty for LAI corresponds to the standard deviation of the measurements (see associated **2014_VGM_ Capitanata.xls** file).*

4.1.3   LI-COR LAI-2000C plant canopy analyser

The LAI-2000C (LI-COR Inc., 2013) is a model of plant canopy analyser used in the field campaign (Figure 5).

Figure 5: LAI-2000C device.

These instruments calculate Leaf Area Index (LAI) and other canopy attributes from light measurements made with a "fish-eye" optical sensor (148º field-of-view). Measurements made above and below the canopy are used to calculate canopy light interception at five

zenith angles (Figure 6). The average probability of light penetration into the canopy is computed by

$$\overline{P(\theta_i)} = \frac{1}{N_{obs}} \sum_{j=1}^{N_{obs}} \frac{B_{ij}}{A_{ij}} \qquad \text{Eq. (5)}$$

where the subscript i (i = 1 … 5) refers to the optical sensor rings centered at θ_i and j refers to the number of observational pairs (j = 1 … N_{obs}). B_{ij} and A_{ij} are the jth below and above canopy readings, respectively, for the ith ring. The gap fraction for the ith ring is computed from

$$G_i = e^{\left(\overline{\ln P(\theta_i)}\right)} = e^{\left(\frac{1}{N_{obs}} \sum_{j=1}^{N_{obs}} \ln \frac{B_{ij}}{A_{ij}}\right)} \qquad \text{Eq. (6)}$$

Assuming the foliage elements are randomly distributed in space, the effective PAI (PAIeff) can be estimated by the transmittance in the different view angles based on Miller's formula (Miller, 1967).

$$PAI_{eff} = 2 \int_0^{\pi/2} - \ln P(\theta) \cos \theta \sin \theta d\theta \qquad \text{Eq. (7)}$$

The amount of foliage in a vegetative canopy can be deduced from measurements of how quickly radiation is attenuated as it passes through the canopy. By measuring this attenuation at several angles from the zenith, foliage orientation information can also be obtained. The LAI-2000 measures the attenuation of diffuse sky radiation at five zenith angles simultaneously, arranged in concentric rings.

A normal measurement with the LAI-2000 consists of a minimum of ten numbers: five of the numbers are the signals from the five detectors when the optical sensor was above the vegetation, and the remaining five are the readings made with the sensor below the vegetation. For both readings, the sensor is looking up at the sky. Five values of canopy transmittance are calculated from these readings by dividing corresponding pairs.
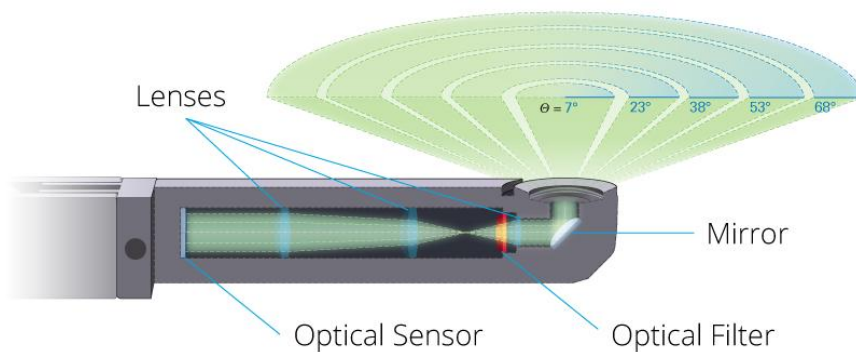
Figure 6: LAI-2000 optical sensor with 5 zenith angles

4.2. SPATIAL SAMPLING SCHEME

A pseudo-regular sampling was used within each Elementary Sampling Unit (ESU) of approximately 10 m by 10 m size within a polygon of 3 km by 3 km size. The two surveys were carried out on March 18-20, 2014 and on May 9-13, 2014. At the first date, 35 fields were monitored: 1 bare soil, 1 artichoke (Figure 7.a), 4 field beans (Figure 7.b) and 29 durum wheat (Figure 7.c). The wheat crop was at elongation stage (Figure 7.d).

For each ESU, the measurement was performed once above the canopy, to obtain reference values, and four times below the canopy, before being averaged out. The four measurements were carried out at the corners of 10m x 10m squares, whose centre georeferenced was used as representative of the ESU where the measurements were performed. The standard error of the four LAI measurements is also given in the instrument output (JECAM, 2014)

a)   b)   c)   d)
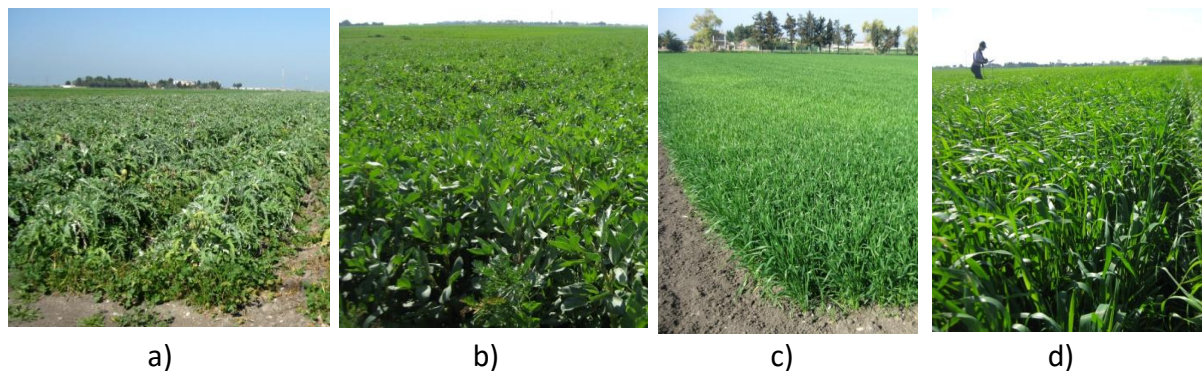
Figure 7: Photos of artichoke (a), field beans (b) and wheat (c and d) in March 2014.

At the second date, 31 fields were monitored, 1 bare soil, 1 artichoke, 4 field beans and 25 durum wheat. The wheat was at milk maturity stage (Figure 8).

a)   b)   c)
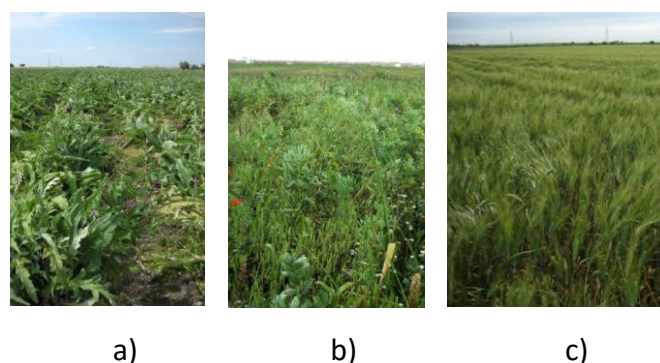
Figure 8: Photos of artichoke (a), field beans (b) and wheat (c) in May 2014.

The spatial sampling over the study area (Figure 9) is located in the middle of Capitanata plain and has a flat topography (avg. altitude 90 m). It keeps most of the properties previously described. The surveyed area is mostly characterized by small-medium farms of 20-ha size on average, intensively cultivated under irrigation regime. Winter durum wheat (Triticum durum Desf.) represents the main cereal crop (about 70% of fields crop area) often grown in rotations with irrigated horticultural species, mainly processing tomato.

According to the local crop management scheduling, durum wheat is usually sown between November and the end of December and harvested in mid June. Another annual main crop of the region is sugar beet (sown in autumn and harvested in July), whereas permanent crops with a significant presence in the area are vineyards and olives trees. (JECAM report 2014).
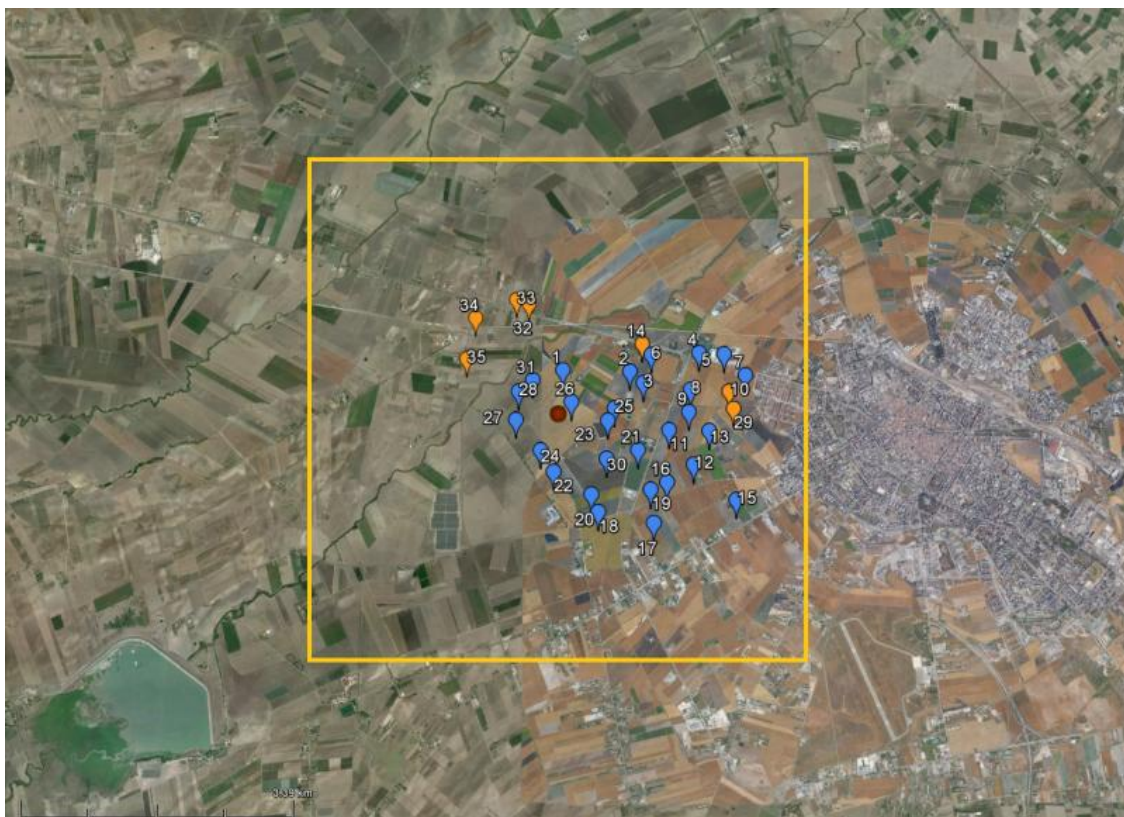
Figure 9: Spatial sampling over the study area of *Capitanata* site located in Italy during the 2014 year. Orange dots: first campaign; Blue dots: second campaign. Most of the samples ESUs of the second campaign are the same as the sampled ESUs of the first campaign, then the oranges are behind the blues.

4.3. GROUND DATA

4.3.1. Data processing

Figure 10 shows the intercomparison between LAI and effective LAI with instantaneous FAPAR. The exponential trend according to Beer's law is observed.
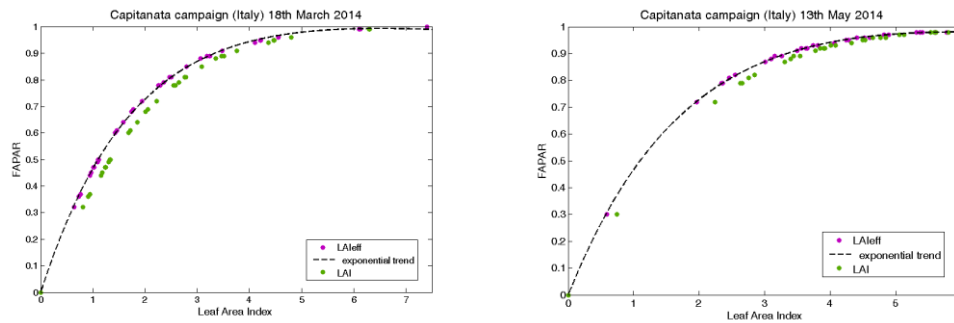
Figure 10: Intercomparison of the measured biophysical variables over the ESUs. Effective LAI and LAI versus FAPAR, *Capitanata* site (Italy). Left side: First field campaign (18th March). Right side: Second field campaign (13th May).

4.3.2. Content of the Ground Dataset

Each ESU is described according to a standard format. The header of the database is shown in **Erreur ! Source du renvoi introuvable.**.

Table 2: The Header used to describe ESUs with the ground measurements.

Column	Var.Name		Comment
1	Plot #		Number of the field plot in the site
2	Plot Label		Label of the plot in the site
3	ESU #		Number of the Elementary Sampling Unit (ESU)
4	ESU Label		Label of the ESU in the campaign
5	Northing Coord.		Geographical coordinate: Latitude (⁰), WGS-84
6	Easting Coord.		Geographical coordinate: Longitude (⁰), WGS-84
7	Extent (m) of ESU (diameter)		Size of the ESU [1]
8	Land Cover		Detailed land cover
9	Start Date (dd/mm/yyyy)		Starting date of measurements
10	End Date (dd/mm/yyyy)		Ending date of measurements
11	Products*	Method	Instrument
12		Nb. Replications	Number of Replications
13		PRODUCT	Methodology
14		Uncertainty	Standard deviation

*LAIeff, LAI and FAPAR

Figure 11 shows the biophysical parameters obtained during the field experiment. Note that additional ESU control points (ECP) were selected by visual inspection (LAIeff, LAI, FAPAR estimated equal to zero, water and urban areas).
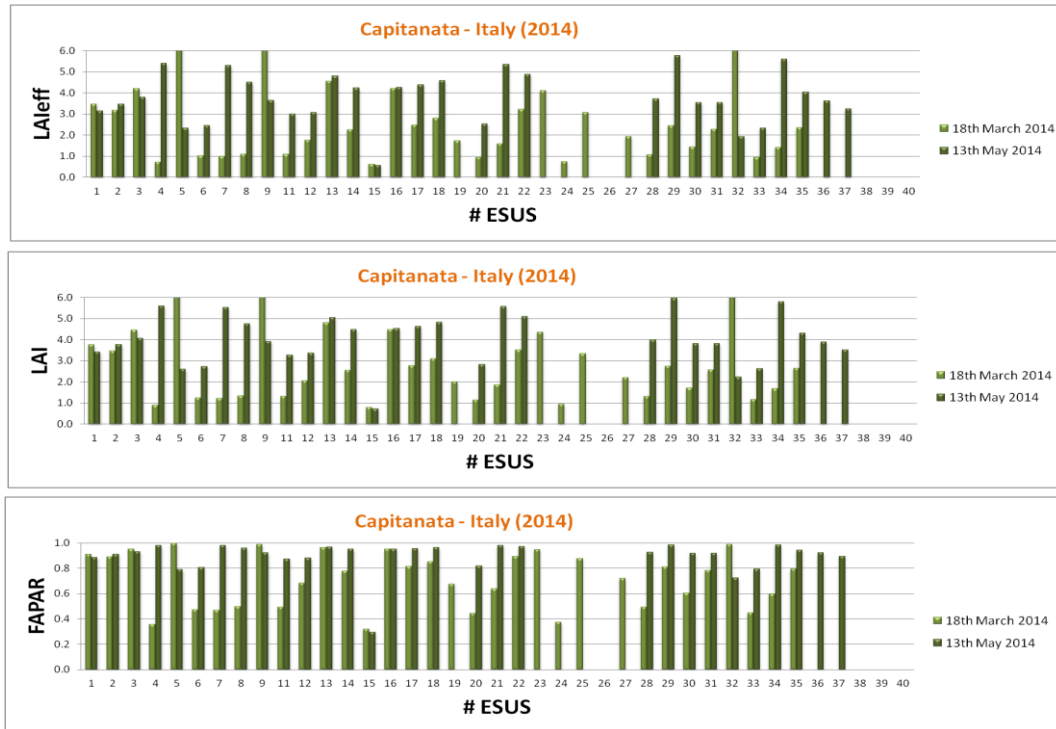
Figure 11: LAIeff, LAI and FAPAR measurements acquired in Capitanata site, during the field campaigns in March and May, 2014.

The distribution of the measured variables is presented in Figure 12 and Figure 13. Note that the larger frequencies are obtained for highest vegetation values for the second campaign (May 2014). For LAI and LAIeff, the first campaign ranges from zero to six.
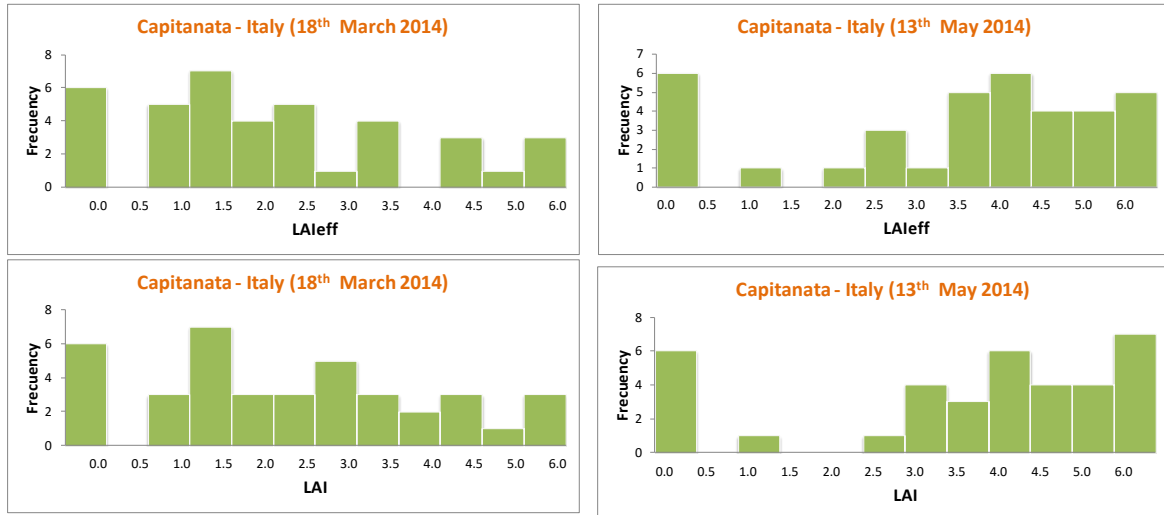
Figure 12: Distribution of the measured biophysical LAIeff and LAI variables over the ESUs, *Capitanata* site, during the field campaigns on 18th March (left) and 13th May, 2014 (right).
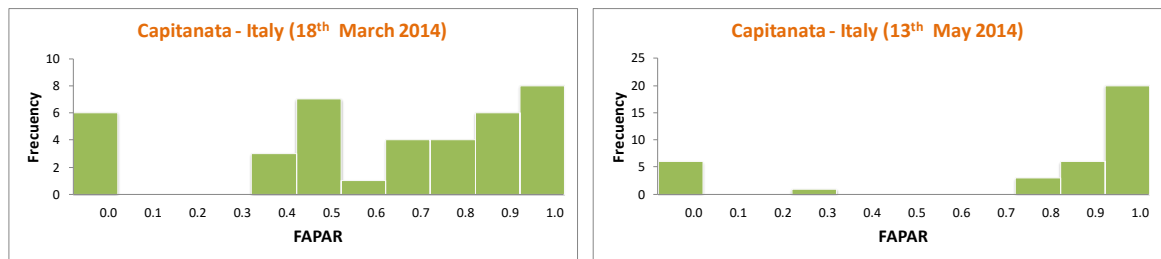
Figure 13: Distribution of the measured biophysical FAPAR variable over the ESUs, *Capitanata* site, during the field campaigns 18th March (left) and 13th May, 2014 (right).

5. EVALUATION OF THE SAMPLING

5.1. PRINCIPLES

The data set sampling was concentrated in the most representative areas, the number of sampling points was 35 and 31, for the first and second field campaign respectively.

5.2. EVALUATION BASED ON NDVI VALUES

The sampling strategy is evaluated using the Landsat-7 image by comparing the NDVI distribution over the site with the NDVI distribution over the ESUs (Figure 14). As the number of pixels is drastically different for the ESU and whole site (WS), it is not statistically consistent to directly compare the two NDVI histograms. Therefore, the proposed technique consists in comparing the NDVI cumulative frequency of the two distributions by a Monte-Carlo procedure which aims at comparing the actual frequency to randomly shifted sampling patterns. It consists in:

1. computing the cumulative frequency of the N pixel NDVI that correspond to the exact ESU locations; then, applying a unique random translation to the sampling design (modulo the size of the image)

2. computing the cumulative frequency of NDVI on the randomly shifted sampling design

3. repeating steps 2 and 3, 199 times with 199 different random translation vectors.

This provides a total population of N = 199 + 1(actual) cumulative frequency on which a statistical test at acceptance probability 1 - α = 95% is applied: for a given NDVI level, if the actual ESU density function is between two limits defined by the $N\alpha/2$ = 5 highest and lowest values of the 200 cumulative frequencies, the hypothesis assuming that WS and ESU NDVI distributions are equivalent is accepted, otherwise it is rejected.
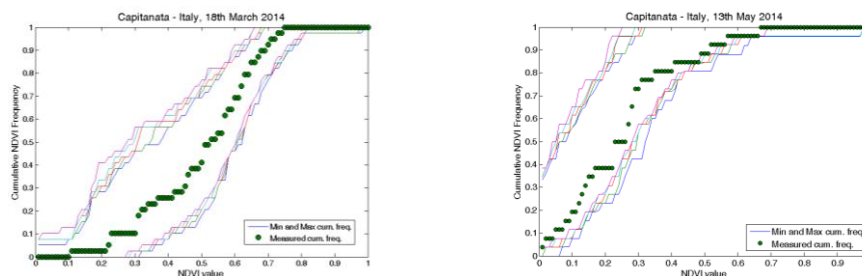

Figure 14: Comparison of NDVI TOA distribution between ESUs (green dots) and over the whole image (blue line). Capitanata site (2014). Left: First field campaign (18th March). Right: Second field campaign (13th May).

Figure 14 shows that the NDVI TOA distribution of the sampling performed during the Capitanata field campaigns is good over the whole site (10x10 km^2) for the two field campaigns. However, for the second campaign (13th May, 2014) a slight bias toward higher NDVI values is appreciated.

5.3. EVALUATION BASED ON CONVEX HULL: PRODUCT QUALITY FLAG.

The interpolation capabilities of the empirical transfer function used for up-scaling the ground data using decametric images is dependent of the sampling (Martinez et al., 2009). A test based on the convex hulls was also carried out to characterize the representativeness of ESUs and the reliability of the empirical transfer function using the different combinations of the selected bands (green, red, NIR and SWIR) of the Landsat-7 image. A flag image is computed over the reflectances. The result on convex-hulls can be interpreted as:

● pixels inside the 'strict convex-hull': a convex-hull is computed using all the Landsat-7 reflectances corresponding to the ESUs belonging to the class. These pixels are well represented by the ground sampling and therefore, when applying a transfer function the degree of confidence in the results will be quite high, since the transfer function will be used as an interpolator;

● pixels inside the 'large convex-hull': a convex-hull is computed using all the reflectance combinations (±5% in relative value) corresponding to the ESUs. For these pixels, the degree of confidence in the obtained results will be quite good, since the transfer function is used as an extrapolator (but not far from interpolator);

● pixels outside the two convex-hulls: this means that for these pixels, the transfer function will behave as an extrapolator which makes the results less reliable. However, having a priori information on the site may help to evaluate the extrapolation capacities of the transfer function.

Figure 15 shows the results of the Convex-Hull test (i.e., Quality Flag image) for Capitanata site over a 10x10 km^2 areas around the central coordinate site. The strict and large convex-hulls are dominant around the test site, 96% and 81% over the 10x10 km^2 area and 99% and 83% for 5x5 km^2 area, first and second field campaign respectively (see

Table 3).

Capitanata site 2014
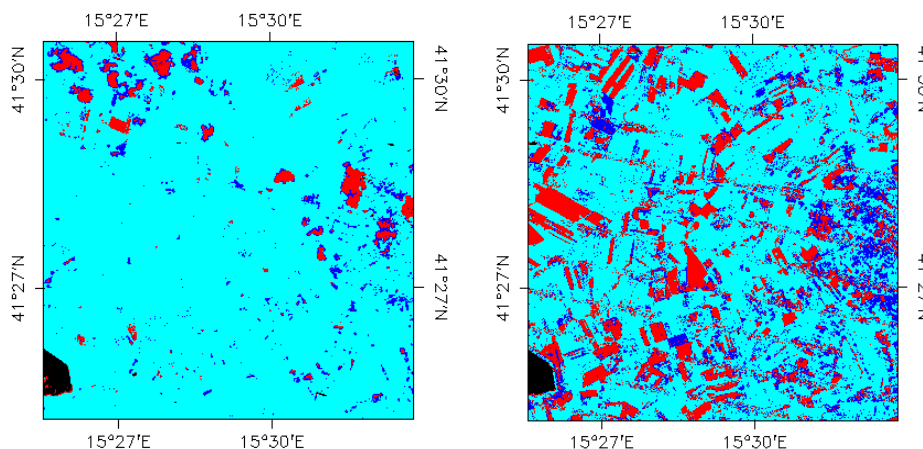
Figure 15: Convex Hull test over 10x10 km^2 area: clear and dark blue correspond to the pixels belonging to the 'strict' and 'large' convex hulls. Red corresponds to the pixels for which the transfer function is extrapolating and black to water areas, *Capitanata* 2014. Top: First field campaign (18th March). Bottom: Second field campaign (13th May).

Table 3: Percentages of Convex hull results over the study areas (10x10 km^2 and 5x5 km^2) in Capitanata, 2014. Convex hull values: 0= extrapolation of TF, 1= strict convex hull and 2= large convex hull.

Capitanata campaigns	Quality Flags (%)						
Field campaigns	**5x5 km^2**				**10x10 km^2**		
	0	**1**	**2**	**1 & 2**	**0**	**1**	**2**
18th March 2014	1	97	2	99	3	93	4
13th May 2014	17	73	10	83	18	68	12

The study area is focused over the 5x5 km^2 area around the central coordinate site. The large image of 100 km^2 includes a part of urban area (Foggia city) and the reservoir of Celone River. Several masks have been created in order to remove this water area, punctual clouds and shadows using the SWIR bands and NDVI. These pixels have been set to -1 for all the products. The area of 3x3 km^2 where the means values of biophysical maps have been calculated is clear and only includes crop fields.

6. PRODUCTION OF GROUND-BASED MAPS

6.1. IMAGERY

The Landsat-7 images were acquired the 2nd March and 21st May, 2014 (see **Erreur ! Source du renvoi introuvable.** for acquisition geometry). We selected 4 spectral bands from 500 nm to 1750 nm with a nadir ground sampling distance of 30 m. For the transfer function analysis, the input satellite data used is Top of Atmoshphere (TOA) reflectance. The original projection is UTM 33 North, WGS-84.

Table 4: Acquisition geometry of Landsat-8 data used for retrieving high resolution maps.

Landsat-8 TOC METADATA		
Platform / Instrument	Landsat-7 / ETM	
Path	189	
Row	31	
Selected Bands	B3(green) : 0.52-0.60 µm B4(red) : 0.63-0.69 µm B5(NIR) : 0.77-0.90 µm B6(SWIR1) : 1.55-1.75 µm	
	Capitanata campaigns	
	18th March 2014	**13th May 2014**
Acquisition date	2014.03.02 9:37:46	2014.05.21 9:38:23
Illumination Azimuth angle	150.6164º	136.8534º
Illumination Elevation angle	36.6060º	62.9371º

As all Landsat-7 scenes collected since May of 2003 have data gaps, it is needed to perform a correction. A number of methods have been used to fill the gaps of Landsat-7 data. Based on the assumption that the same-class neighboring pixels exhibit similar patterns of spectral differences between dates, we used a simple and effective method to interpolate the values of the pixels within the gaps. This method is the Neighborhood Similar Pixel Interpolator (NSPI). Results indicate that NSPI can restore the value of un-scanned pixels very accurately, and that it works especially well in heterogeneous regions (Chen et al., 2011; Latorre et al., 2014).

Figure 16 shows a vertical profile of the Landsat-7 image, before and after the gap filling correction. The profiles show a good restoration for all bands, the figure corresponds to the NIR band.
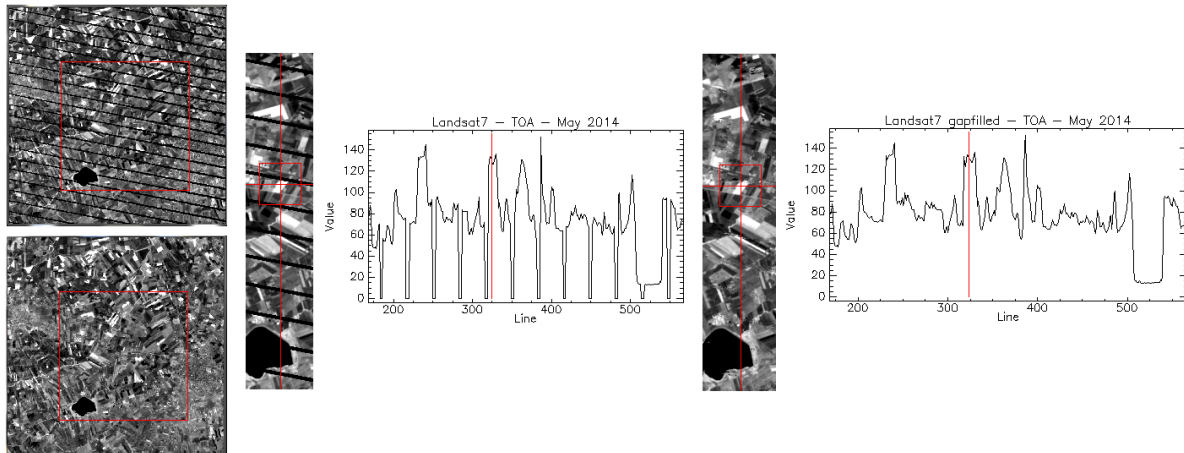
Figure 16: Vertical profile over the *Capitanata* site, for NIR band of original Landsat-7 image (Left) and gap filled Landsat-7 image (Right). 2nd March, 2014.

6.2. THE TRANSFER FUNCTION

The measurements were collected in different dates that the acquisition dates of the Landsat-7 images used for the up-scaling. For this reason some measurements provided in the ground dataset present inconsistent values with the TOA reflectance and NDVI values of the satellite image. These measurements, corresponding to few ESUs were not considered for the transfer function.

6.2.1. The regression method

If the number of ESUs is enough, multiple robust regression 'REG' between ESUs reflectance and the considered biophysical variable can be applied (Martínez et al., 2009): we used the 'robustfit' function from the Matlab statistics toolbox. It uses an iteratively re-weighted least squares algorithm, with the weights at each iteration computed by applying the bi-square function to the residuals from the previous iteration. This algorithm provides lower weight to ESUs that do not fit well.

The results are less sensitive to outliers in the data as compared with ordinary least squares regression. At the end of the processing, two errors are computed: weighted RMSE (using the weights attributed to each ESU) (RW) and cross-validation RMSE (leave-one-out method) (RC).

As the method has limited extrapolation capacities, a flag image (Figure 15), based on the convex hulls, is included in the final ground based map in order to inform the users on the reliability of the estimates.

6.2.2. Band combination

Figure 17 shows the errors (RW, RC) obtained for the several band combinations using TOA reflectance for the first (left) and the second campaign (right). We have selected the NDVI as input for the transfer function (exponential relationship with LAI and linear relationship with FAPAR, see section 6.2.3). NDVI shows in most cases the lower errors over ESUs than other combinations and assures good consistency of the maps over the whole area.
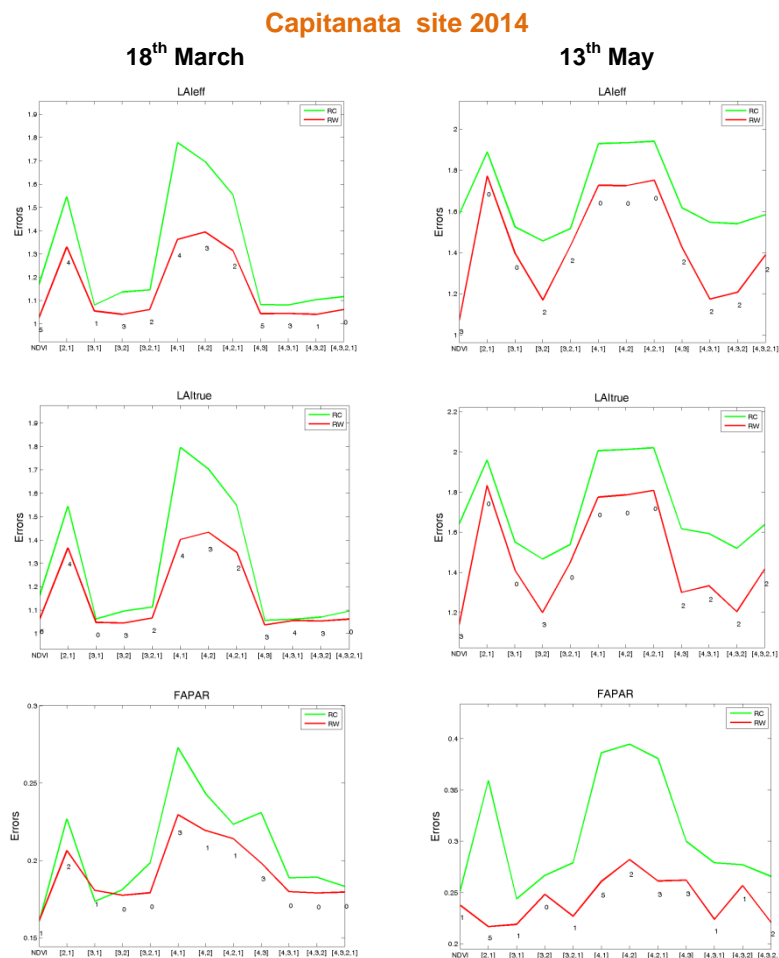
Figure 17: Test of multiple regression (TF) applied on different band combinations. Band combinations are given in abscissa (1=G, 2=RED, 3=NIR and 4=SWIR). The weighted root mean square error (RMSE) is presented in red along with the cross-validation RMSE in green. The numbers indicate the number of data used for the robust regression with a weight lower than 0.7 that could be considered as outliers. *Capitanata* 2014, first field campaign on 18th March and 13th May.

6.2.3. The selected Transfer Function

The applied transfer function is detailed inTable 5, along with its weighted (RW) and cross validated (RC) errors.

For the FAPAR, a simple linear relationship with NDVI was selected:

$$FAPAR = a + b \cdot NDVI \qquad \text{Eq. (8)}$$

For the LAIeff and LAI, an exponential relationship with NDVI was selected according to Baret et al., (1989):

$$LAIeff = a + b \cdot ln\left(\frac{NDVI_\infty - NDVI}{NDVI_\infty - NDVI_s}\right) \qquad \text{Eq. (9)}$$

$$LAI = a + b \cdot ln\left(\frac{NDVI_\infty - NDVI}{NDVI_\infty - NDVI_s}\right) \qquad \text{Eq. (10)}$$

Where b represents the extinction coefficient which depends on the average leaf angle inclination, solar zenith angle and diffuse reflectance and transmittance of the leaves. "b" was set empirically with the ground data for each transfer function, as well as the residuals "a". $NDVI_s$ represents the typical NDVI of bare soil areas and $NDVI_\infty$ represents the NDVI of fully developed canopies, both assumed to be constant over the image. $NDVI_s$ was set to 0.09 and 0.22 for the first and second campaign, respectively. The values for $NDVI_\infty$ were 0.6 and 0.83.

The results obtained for FAPAR on May were discarded due to the lower correlation (see Figure 18)

Table 5: Transfer function applied to the whole site for LAIeff, LAI and FAPAR. RW for weighted RMSE, and RC for cross-validation RMSE.

Variable	Band Combination	RW	RC
18th March 2014			
LAIeff	$0.3416 - 1.7096 \cdot ln\left(\frac{0.6 - NDVI}{0.6 - 0.09}\right)$	1.03	1.11
LAI	$0.4466 - 1.8377 \cdot ln\left(\frac{0.6 - NDVI}{0.6 - 0.09}\right)$	1.06	1.11
FAPAR	$-0.1231 + 1.3723 \cdot NDVI$	0.16	0.15
13th May 2014			
LAIeff	$1.3794 - 5.5223 \cdot ln\left(\frac{0.83 - NDVI}{0.83 - 0.22}\right)$	1.07	1.57
LAI	$1.4884 - 5.7780 \cdot ln\left(\frac{0.83 - NDVI}{0.83 - 0.22}\right)$	1.14	1.62

Figure 18 shows scatter-plots between ground observations and their corresponding transfer function (TF) estimates for the selected bands combinations. A good correlation is observed for the LAIeff, LAI and FAPAR with points distributed along the 1:1 line. Note that FAPAR for the second campaign displayed poor results, with low correlation for high ground FAPAR values. As a result, for this second campaign, the up-scaled FAPAR maps were found not reliable, and they are not provided.-
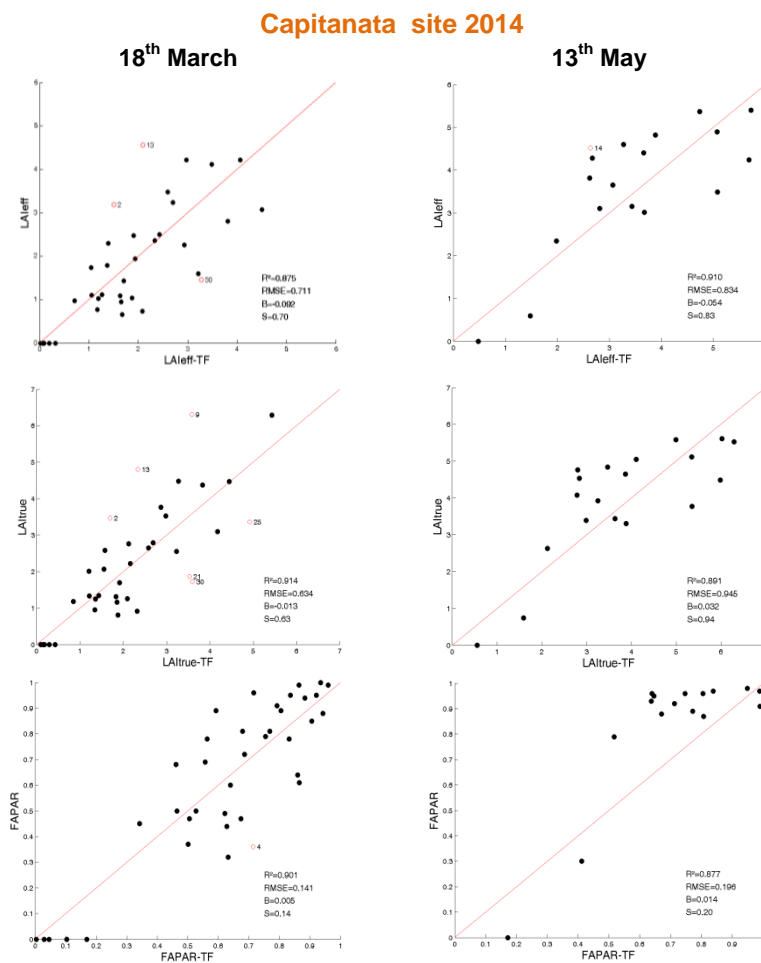

Figure 18: LAIeff, LAI and FAPAR results for regression on reflectance using the NDVI band. Full dots: Weight>0.7. Empty dots: 0<Weight<0.7. Crosses: Weight=0. Capitanata site 2014, field campaigns on 18th March and 13th May. Note that FAPAR-TF for the second campaign (May) is not provided due to its poor results.

6.3. THE HIGH RESOLUTION GROUND BASED MAPS

The high resolution maps are obtained applying the selected transfer function (Table 5) to the Landsat-7 TOA reflectance. The study area has been extended to 10x10km^2 (centre located at 41.4637 N, 15.4867 E, UTM zone 33 North, Datum WGS-84). Figure 19 to Figure 21 present the TF biophysical variables over the extended 10x10 km^2 area. Figure 15 shows the Quality Flag included in the final product.
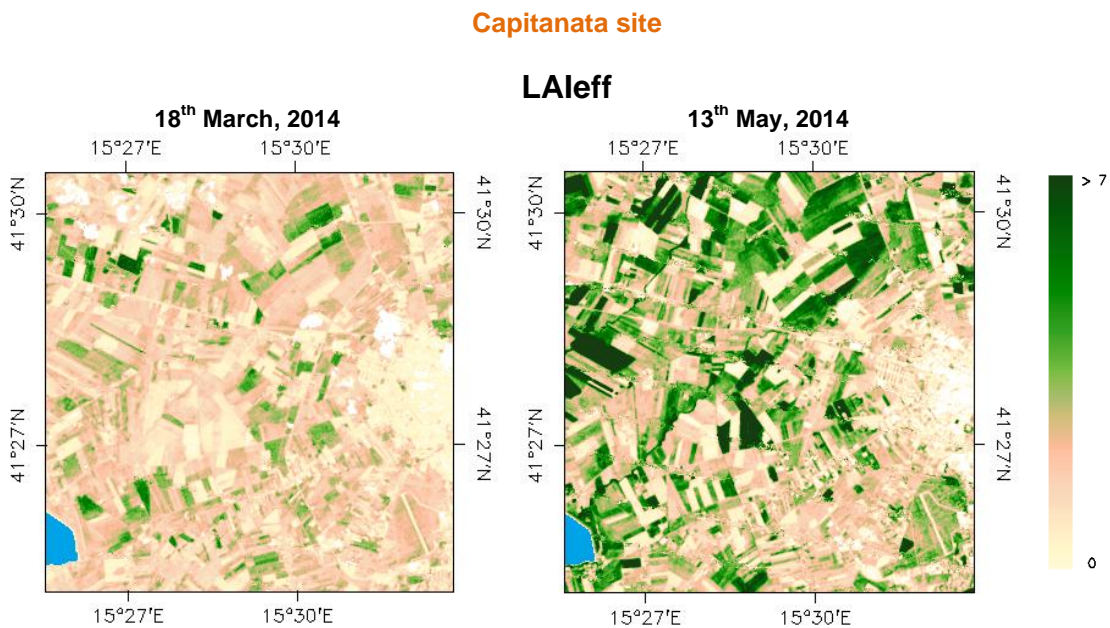
Capitanata site

Figure 19: Ground-based Effective LAI maps (10x10 km^2) retrieved on *Capitanata site (Italy) 2014.* Left: First field campaign (18th March). Right: Second field campaign (13th May).

Capitanata site

LAI

18th March, 2014   **13th May, 2014**
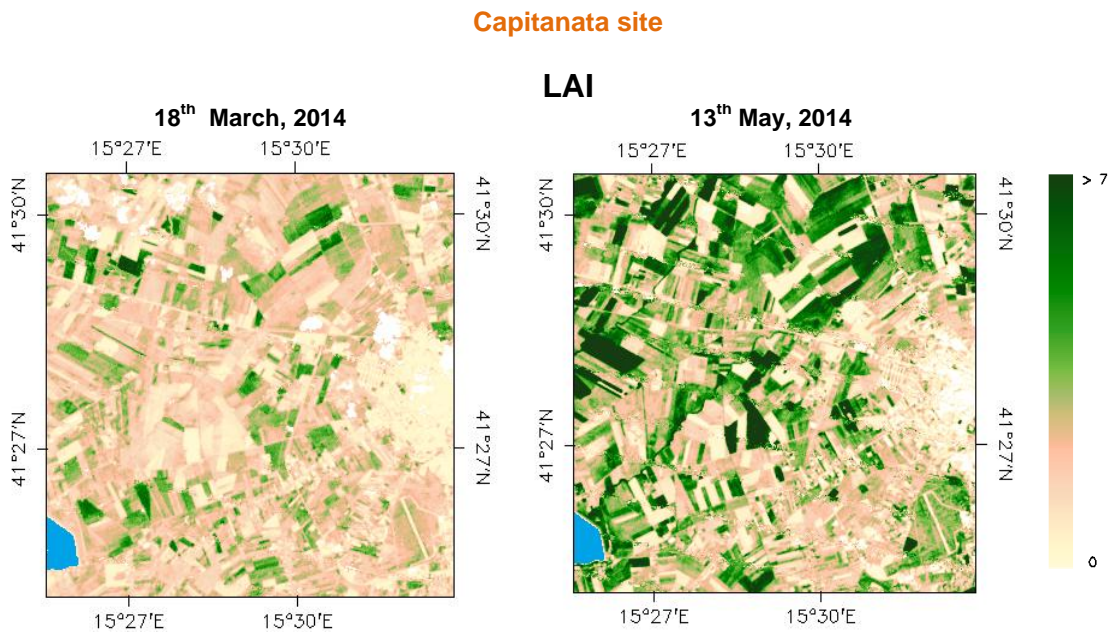

Figure 20: Ground-based LAI maps (10x10 km2) retrieved on *Capitanata site (Italy) 2014.* Left: First field campaign (18th March). Right: Second field campaign (13th May).
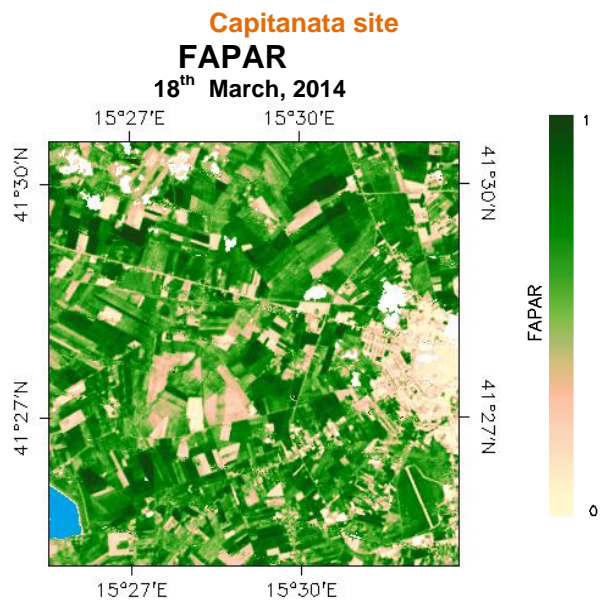
Capitanata site
FAPAR
18th March, 2014

Figure 21: Ground-based of Instantaneous FAPAR maps (10x10 km2) retrieved on *Capitanata site (Italy) 2014.* First field campaign (18th March).

Figure 22 and Figure 23 shows these ground-based high resolution maps over the 5x5 km^2 study area.

Capitanata site 18th March, 2014

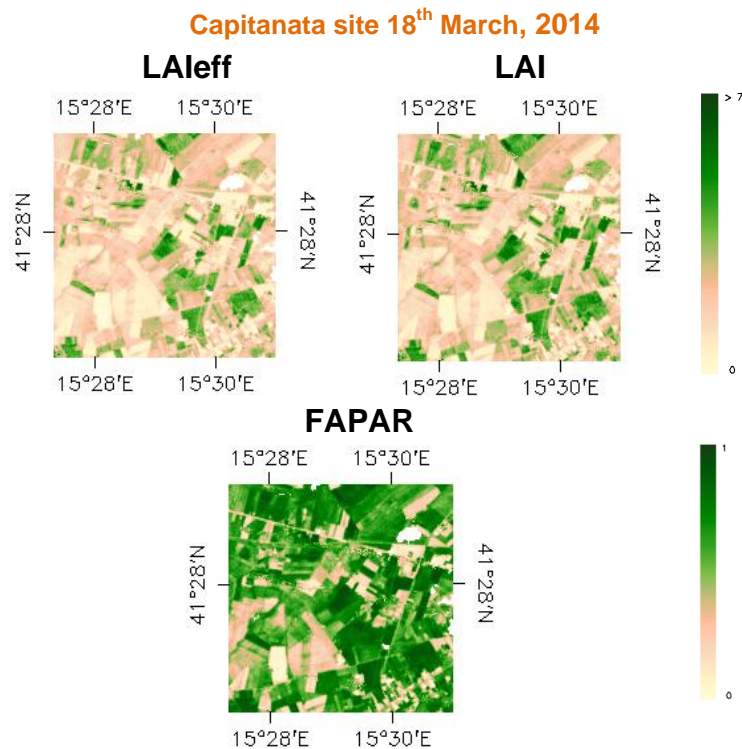**Figure 22: Ground-based maps (5x5 km^2) retrieved on the Capitanata site (Italy). First field campaign on 18th March, 2014.**

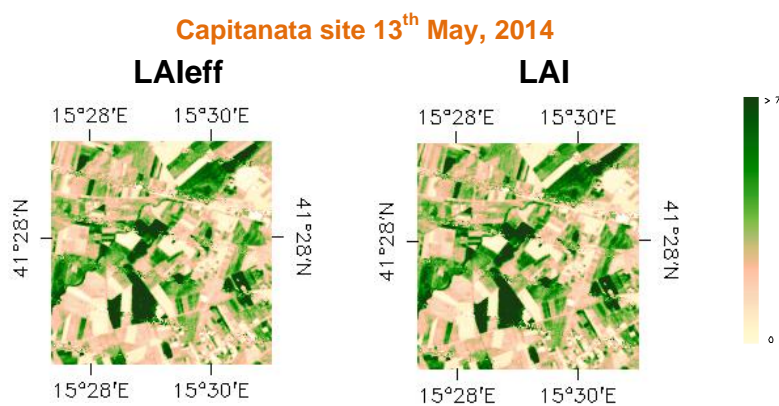**Capitanata site 13th May, 2014**

Figure 23: Ground-based maps (5x5 km^2) retrieved on Capitanata site (Italy). Second field campaign on 13th May, 2014.

Figure 24 shows a scatter plot between biophysical variables that prove the good consistency of the 10x10 km^2 ground-based maps (all pixels), showing the exponential (LAI vs FAPAR) observed with the ground data.

Capitanata site 2014
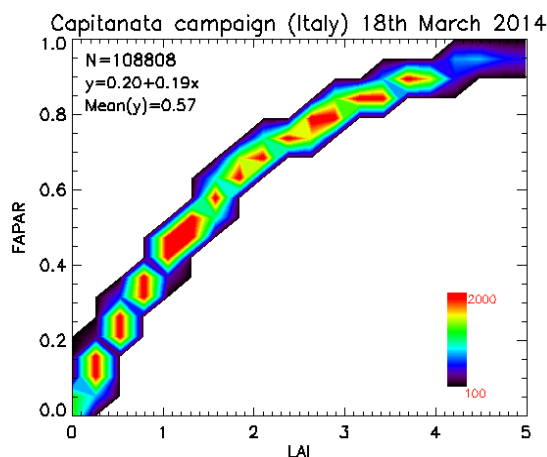
LAI vs FAPAR
18th March, 2014

Figure 24: Scatter plots to LAI vs FAPAR for the first field campaign (18th March) over Capitanata site (Italy) 2014.

6.3.1. Mean Values

Mean values of a 3x3 km^2 area centred in the test site are provided for the validation of 1 km satellite products in agreement with the CEOS OLIVE direct dataset (Table 6). For the validation of coarser resolutions product (e.g. MSG products) a larger area should be considered. For this reason, empirical maps are provided at 5x5 km^2 and 10x10 km^2.

Table 6: Mean values and standard deviation (STD) of the HR biophysical maps for the selected 3 x 3 km^2 areas at Capitanata site (Italy) 2014.

3x3 km^2	Capitanata campaigns 2014					
	Mean Values			STDV Values		
	LAIeff	LAI	FAPAR	LAIeff	LAI	FAPAR
18th March 2014	1.62	1.82	0.56	0.99	1.06	0.22
13th May 2014	2.93	3.08	-	1.99	2.01	-

Table 7 describes the content of the geo-biophysical maps in the "BIO_YYYYMMDD_LANDSAT7_Capitanata_ETF_10x10" files.

Nomenclature: BIO_YYYYMMDD_SENSOR_Site_ETF_Area
where:

BIO stands for Biophysical (LAIeff, LAI and FAPAR)

SENSOR = LANDSAT7

YYYYMMDD = Campaign date

Site = Capitanata

ETF stands for Empirical Transfer Function

Area = window size 10x10 and 5x5

Table 7: Content of the dataset.

Parameter	Dataset name	Range	Variable Type	Scale Factor	No Value
LAI effective	LAIeff	[0, 7]	Integer	1000	-1
LAI	LAI	[0, 7]	Integer	1000	-1
FAPAR 10:00 SLT	FAPAR	[0, 1]	Integer	10000	-1
Fraction of Vegetation Cover	FCOVER	[0, 1]	Integer	10000	-1
Quality Flag	QFlag	0,1,2,3 (*)	Integer	N/A	-1

[*] 0 means extrapolated value (low confidence), 1 strict interpolator (best confidence), 2 large interpolator (medium confidence), 3 mask for water areas.

7. CONCLUSIONS

The FP7 ImagineS project continues the innovation and development activities to support the operations of the Copernicus Global Land service. One of the JECAM sites is located in the northern part of Apulia Region (South-eastern Italy), the study is focused on an experimental farm situated in the middle of Capitanata plain within a flat topography (avg. Altitude 90 m) in Italy.

This report firstly presents the ground data collected during two field campaigns on 18th of March and 13th of May, 2014. The dataset includes 35 and 31 elementary sampling units where LAIeff measurements were taken with the analyzer LAI2000 and LAI and FAPAR values were obtained with empirical relationships. Clumping Factor was empirically determined using the using the Rinaldi and Garofalo, (2011) expression. Solar Global Radiation was collected with pyranometer. iPAR was estimated using Rinaldi and Garofalo, (2011) method over the ESUs.

Secondly, high resolution ground-based maps of the biophysical variables have been produced over the site. Ground-based maps have been derived using high resolution imagery (Landsat-7 TOA Reflectance) according to the CEOS LPV recommendations for validation of low resolution satellite sensors. Transfer functions have been derived by multiple robust regressions between ESUs reflectance and the several biophysical variables. We have selected the NDVI as input for the transfer function (exponential relationship with LAIeff and LAI, linear with FAPAR). NDVI assures good consistency of the maps over the whole area, and provides the lowest RMSE error in most cases. The RMSE values for the several transfer function estimates are 0.71 and 0.83 for LAIeff, 0.63 and 0.95 for LAI, and 0.14 for FAPAR. Note that for the second campaign, the transfer function results for FAPAR are not provided due to the low correlation obtained between ground and satellite estimates.

The quality flag map based on the convex-hull analysis shows quite good quality (upper than 83% at 5x5 km^2 and 81% at 10x10 km^2).

The biophysical variable maps are available in geographic (UTM 33 North projection WGS-84) coordinates at 30 m resolution. Mean values and standard deviation for LAIeff, LAI, and FAPAR were computed over an area of 3x3 km^2 for validation of low and medium resolution satellite products.

8. ACKNOWLEDGEMENTS

9. REFERENCES

Baret, F and Fernandes, R. (2012). Validation Concept. VALSE2-PR-014-INRA, 42 pp.

Baret, F., G. Guyot and Major, D. (1989). Crop biomass evaluation using radiometric measurements. Photogrammetria 43:241-256.

Camacho, F., Cernicharo, J., Lacaze, R., Baret, F., and Weiss, M. (2013). GEOV1: LAI, FAPAR Essential Climate Variables and FCOVER global time series capitalizing over existing products. Part 2: Validation and intercomparison with reference products. *Remote Sensing of Environment, 137: 310-329.*

Chen, J., Zhu X., Vogelmann J. E., Gao F., Jin S. (2011). A simple and effective method for filling gaps in Landsat ETM+ SLC-off images. Remote sensing of environment. 115: 1053-1064.

Decagon Devices, Inc. (2014). AccuPAR PAR/LAI Ceptometer. Model LP80 manual. http://www.decagon.com

Demarez, V., Duthoit, S., Baret, F., Weiss, M. and Dedieu, G. (2008). Estimation of leaf area and clumping indexes of crops with hemispherical photographs. *Agricultural and Forest Meteorology. I48, 644-655.*

Fernandes, R., Plummer, S., Nightingale, J., et al. (2014). Global Leaf Area Index Product Validation Good Practices. CEOS Working Group on Calibration and Validation - Land Product Validation Sub-Group. *Version 2.0: Public version made available on LPV website.*

JECAM, 2014, Progress Report 2014 (available online: http://www.jecam.org/images/uploads/sites/JECAM_Progress_Report_2014_.pdf)

Lang A.R.G., (1986). Leaf area and average leaf angle from transmittance of direct sunlight. Australian Journal of Botany. 34: 349-355

Lang, A.R.G., (1987). Simplified estimate of leaf area index from transmittance of the sun's beam. Agricultural and Forest Meteorology. 41: 179-186

Latorre, C., Camacho, F., Piñó, C., Kussul, N., Serhiy, S., Koloti, A., Shelestov, A. (2014). "Vegetation Field Data and Production of Ground-Based Maps: 12th June, 31st July. Pshenichne site, Ukraine" report. (Available at ImagineS website: http://fp7-imagines.eu/pages/documents.php).

LI-COR Inc., Lincoln, Nebraska, (2013). http://envsupport.licor.com/docs/LAI-2000_Instruction_Manual.pdf

Martínez, B., García-Haro, F. J., & Camacho, F. (2009). Derivation of high-resolution leaf area index maps in support of validation activities: Application to the cropland Barrax site. *Agricultural and Forest Meteorology, 149, 130–145.*

Miller, J.B. (1967). A formula for average foliage density. Aust. J. Bot., 15:141-144

Morisette, J. T., Baret, F., Privette, J. L., Myneni, R. B., Nickeson, J. E., Garrigues, S., et al. (2006). Validation of global moderate-resolution LAI products: A framework proposed within the CEOS land product validation subgroup. *IEEE Transactions on Geoscience and Remote Sensing, 44, 1804–1817*.

Nilson T. (1971). A theoretical analysis of the frequency of gaps in plant stands. Agricultural Meteorology 8, 25-38

Rinaldi, M., Garofalo, P., (2011). Radiation-use efficiency of irrigated biomass sorghum in a Mediterranean environment. Crop Pasture and Science, 62:830-839.